PRESENT STATUS AND FUTURE PROSPECT ON THE INITIAL REALIGNMENT AT THE KEKB INJECTOR LINAC

T. Suwada*, T. Higo, K. Kakihara, T. Kamitani, M. Satoh, R. Sugahara, M. Tanaka,
KEK, Tsukuba, Japan

Abstract

The initial realignment of beam lines is in progress at the KEKB injector linac; the realignment was necessitated by the Great East Japan Earthquake of March 2011 and is a requirement for the Super KEK B-factory project (SuperKEKB). Two alignment methods are applied to the initial realignment. One is a laser-based alignment technique applied to the two long straight sections. By using this technique, the transverse displacements of the accelerator girder units along the two long straight sections have been independently aligned with respect to two different laser axes. The other technique involves the use of a conventional laser tracker, and it is applied to the alignment of the components (accelerating structures and magnets) installed on the girder units and in the 180° arc section. A series of measurements provide an accurate view of the high-precision alignment of the linac beam line using the two alignment techniques. Regarding the component alignment, target bases for the accelerator structures and quadruple magnets have been newly fabricated and mounted for measuring the laser-tracker-based alignment. The girder units have been improved to increase their earthquake resistance by mounting a new support table for restricting their displacements in both the transverse and axial directions. For the alignment of the 180° arc section, refinement has been performed to connect the arc smoothly with the two straight sections. We have observed a non-negligible long-term drift of the tunnel floor along with a daily range of dynamical displacements due to tidal motion. We are now preparing a remote-controlled measurement system of the floor level to investigate the cause of such dynamical motion. This report contains a detailed description of the present status and future prospect of the initial realignment at the KEKB injector linac.

INTRODUCTION

The SuperKEKB [1] is a next-generation B-factory that has been under construction at KEK since the KEK B-factory [2] was discontinued in 2010. The SuperKEKB is an electron/positron collider with asymmetric energies, and it comprises 4-GeV positron (LER) and 7-GeV electron (HER) rings with stored beam currents of 3.6 A and 2.6 A, respectively. The target luminosity ($8\times10^{35}/\mathrm{cm}^2/\mathrm{s}$) will be 40 times the peak luminosity of the previous KEKB. The motivation for construction the SuperKEKB is the urgent need to perform high-energy flavor physics experiments concerning the CP violation in B mesons [3].

* tsuyoshi.suwada@kek.jp

The KEKB injector linac [4] is a linear accelerator (linac) for both the SuperKEKB and two light sources: the Photon Factory (PF) and Photon Factory-Advanced Ring for pulse X-rays (PF-AR). For the aim of the SuperKEKB, the injector linac is being concurrently upgraded for both the aforementioned purposes [5, 6]. The requirements for the injector linac are full energy injection into the SuperKEKB with an energy spread of 0.1%; electron- and positron-beam emittances of 20 and 10 mm·mrad, respectively during the linac operation; bunch charges of 5 and 4 nC, respectively. A low-emittance and high-current electron beam is to be generated by using a new photo-cathode RF gun [7].

The low-emittance and high-current positron beam is to be generated by bombarding a tungsten target with high-energy primary electrons with an energy of 3.5 GeV and electron charges of 10 nC/bunch. The positrons are to be efficiently captured using a new flux concentrator and large aperture S-band accelerating structures [8], which are to be damped to the level required for the low-emittance beam through a new damping ring (DR) [9].

For the injection to the SuperKEKB, the bunch charges should be increased by factors of five and four for electrons and positrons, respectively, and the transverse emittances should be reduced by factors of 15 and 210 without and with a damping ring for electrons and positrons, respectively, in comparison with the previous KEKB. Such a challenging injection scheme requires high-precision alignment of the injector linac.

The laser-based alignment technique is one of several alignment techniques developed for long accelerator complexes [10]. This alignment technique is advantageous as it can not only be applied to alignment measurements for long linacs but can also be used for regular monitoring of the straightness of the linac without any interruption in the operation. This technique has another advantage over other techniques in that a long fiducial straight line could be more definitely implemented. The implementation of a laser beam with high pointing stability, for this purpose, is a challenging task for high-precision alignment measurements in long linacs.

OVERVIEW OF THE KEKB INJECTOR LINAC

A schematic layout of the injector linac and fiducial laser paths for the two long straight sections are shown in fig. 1. The injector linac with a total length of 600 m comprises eight sectors (A–C and 1–5), which together constitute the two long straight sections. One section is 125 m long and is

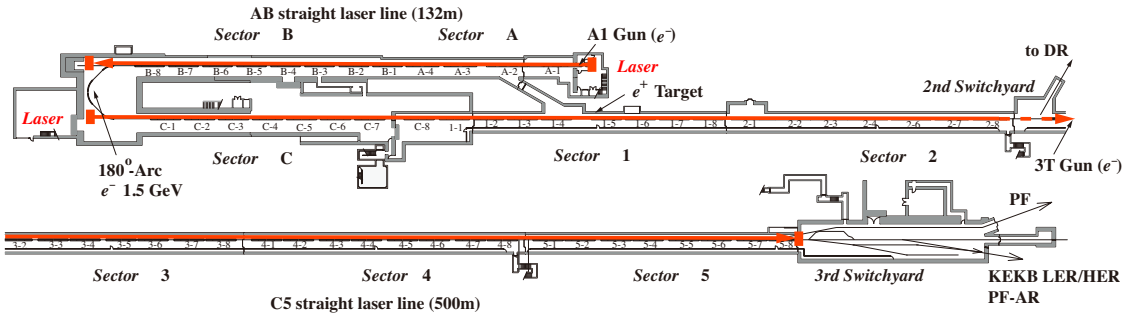

Figure 1: Schematic layout of the injector linac and the fiducial laser paths for the two long straight sections.

composed of sectors A and B; the other is 476 m long and is composed of sectors C and 1–5. These two straight sections are connected to a 180° arc with a diameter of 15 m, where the beam energy is fixed at 1.5 GeV.

Single-bunch electron beams can be generated using an A1 electron gun and passed through a preinjector to attain a pulse width of ∼10 ps. The electron gun can generate electron beams with maximum charges of 20 nC/bunch and a maximum repetition rate of 50 Hz for positron production. The primary electron beams (∼10 nC/bunch) can be stably accelerated to 3.5 GeV from the end of the buncher to a positron production target installed in girder unit 1–5. The positron beams can be accelerated to 1.1 GeV and transported into the new DR through a new beam transport line under construction.

The DR with a circumference length of 136 m is under construction alongside the end section of sector 2 (not shown), and it is to be connected to the linac-to-DR transport line (LTR) at the second beam switchyard (SY2). The positron beams shall be extracted after the damping time of 40 ms from the DR. After the positron beams are delivered from the DR, they shall subsequently be transported back through the DR-to-linac transport line (RTL) to SY2, and again accelerated to 4.0 GeV in the linac end for injection into the SuperKEKB LER. The electron beams shall be directly accelerated to 7 GeV at the linac end for injection into the SuperKEKB HER.

INITIAL REALIGNMENT

Overview

The aim of the initial realignment is to attain alignment precisions of 0.1 mm (rms) and 0.3 mm (rms) in one standard deviation in a local region (typical sector length of ∼80 m) and the entire region of the long straight sections, respectively. A laser-based alignment system with a conventional He-Ne laser has been newly developed for high-precision alignment of the girder units in the long straight sections [10]. The laser beam was first implemented as a 500-m-long fiducial straight line for alignment measurements. We experimentally investigated the propagation and stability characteristics of the laser beam passing through laser pipes in a vacuum of ∼3 Pa. High pointing stability was successfully obtained at the last fiducial point with transverse displacements of 40 μm in one standard deviation by applying a feedback control. This pointing stability corresponds to an angle of 0.08 μrad.

A typical sector is 76.8 m long and comprises eight girder units, each having a length of 9.6 m. The girder unit structure is shown in fig. 2. A typical girder unit is 8.44 m long and is installed at the floor level in the tunnel; four 2-m-long S-band accelerating structures are mounted on the unit. Quadrupole magnets for beam focusing are installed on special magnet girders between the two adjacent girder units. The girder unit is composed of a stainless-steel, earthquake-resistant cylindrical tube (outer diameter: 508 mm) with L-shaped plates attached to both ends; the L-shaped plates support the entire weight (∼1.6 t) of the girder unit. Four accelerating structures are mounted on five separate stainless-steel support plates on the girder unit. These support plates are adjustable in the vertical direction. The electron and positron beams pass through the center holes of the accelerating structures mounted 1.2 m above the floor level. A laser beam passes through the center of the laser pipe installed 780 mm above the floor level. The mechanical structure of the girder unit is reported in detail elsewhere [11].

The accelerating structures are mounted on support plates on which reference guide rails are fixed, and the support plates of the accelerating structure are mechanically attached to the lateral surface of the reference guide rails. The center positions of the four accelerating structures and reference guide rails are aligned using the laser-tracker alignment technique, in which two fiducial points are utilized. The two fiducial points are located at both ends of the girder unit and make a straight line parallel to the laser axis at a horizontal distance of 400 mm where a tracker target is mounted using a new mechanical jig (see fig. 3).

Regarding the component alignment, new target bases for the accelerator structures have been developed to measure the alignment (see fig. 4). The target base is mounted on an outer surface of the rf coupler. The horizontal level of the target base is adjustable with a standard level of precision 0.02 mrad. Other target bases for the quadrupole magnets have also been newly fabricated and mounted. Such alignment procedures in each accelerator unit could be per-

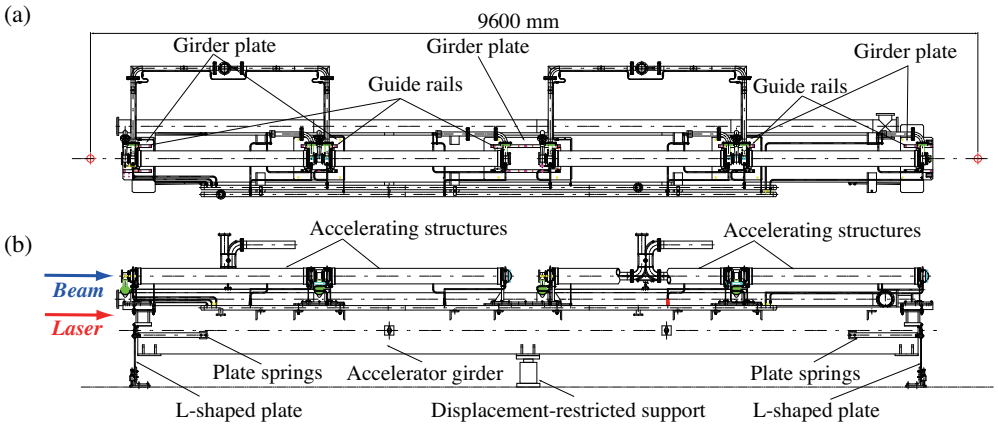

Figure 2: Mechanical drawings of the accelerator girder unit: (a) top view and (b) front view.

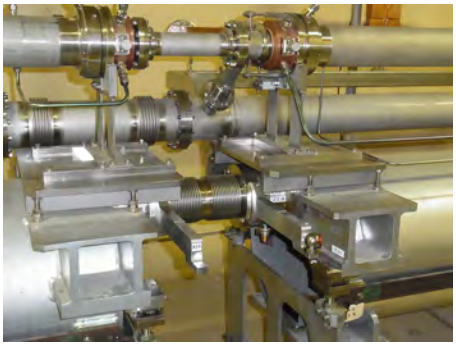

Figure 3: Mechanical jigs for mounting the tracker target. The jig and QPD are connected by high-precision flange-flange mechanical joining.

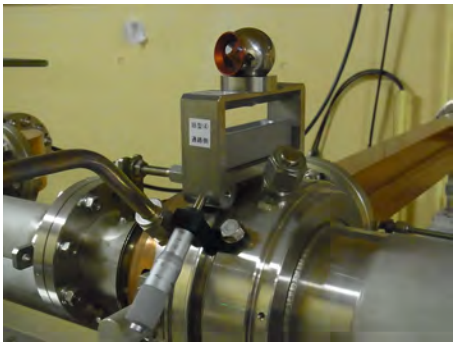

Figure 4: Target base for the laser tracker in the alignment measurement of the accelerating structures.

formed with a precision of 20 μm in one standard deviation in both the horizontal (x) and vertical (y) directions.

Laser-based alignment for long straight sections

This is a conventional laser-based alignment technique with quadrant silicon photodiodes (QPDs). In this alignment technique, a laser straight line is directly considered as a fiducial axis by connecting two (or three) fiducial points. The QPD is located at each target point, which should be aligned, and it is directly irradiated with the laser beam. The center positions of the target point can be estimated by measuring the gravity center of the intensity distribution of the fiducial laser in the transverse directions with the QPD. The girder units could be precisely aligned along the fiducial straight line by measuring their transverse displacements from the fiducial line.

The new laser source and optical lens configuration are the new input optical system is shown in fig. 5.

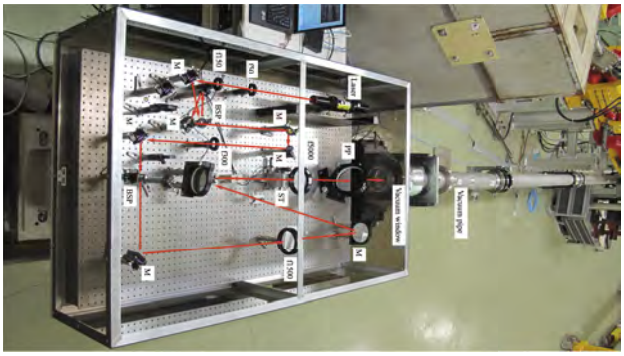

Figure 5: He-Ne laser source and input optical system. PBS: polarizing beam splitter, M: reflection mirror, PP: parallel plate, ST: linear stage.

The input optical system is based on a dioptric system having dioptric lenses and reflecting mirrors. A laser beam with a small dispersion angle is delivered from a 10-mW He-Ne laser tube. The transverse width of the laser beam is W_x (or W_y) $\simeq$ 0.83 mm at a point 10 cm downstream from the frontend face of the laser tube, and its divergence is $\sim$0.7 mrad. Here, it should be mentioned that the beam width is defined by a four-sigma width of the intensity distribution projected onto the x or y axes in the two-dimensional intensity profile. The beam width is slowly expanded to W_x (or W_y) $\simeq$ 29 mm at the outlet of the input optical system by using five spherical plano-convex lenses (BK7, focal lengths: f = 50, 150, 300, 1500, and 5000 mm) mounted on the optical table. The total path

length of the laser beam is ∼5.5 m in the optical table.

The propagation direction of the laser beam should be adjusted to be as precisely parallel to the line joining the two fixed QPDs as possible without any excessive diffraction and instability. The two fixed QPDs are installed just after the input optical system and at the end of the long straight section. The laser beam incident on the vacuum pipes should have adjustable incident angles and transverse positions in both the x and y directions at the input optical system. The incident angles are adjusted by moving the final spherical plano-convex lens ($f5000$) in the plane perpendicular to the beam axis. This lens is mounted on high-precision translation stages with pico-motor actuators, which can control the incident angles with minimum x- and y-angle steps of 1.8 nrad and 0.73 nrad, respectively, via a stage controller. The incident angles can be automatically adjusted with a feedback control. On the other hand, the transverse positions are manually adjusted by tilting a parallel plate located after the final lens. Thus, the transverse positions of the laser beam can be moved roughly and finely without changing any angles.

Currently, the forty girder units from sector A to sector 2 were successfully aligned using the laser-based alignment technique with a precision of less than 0.1 mm.

Laser tracker-based component alignment

Regarding the component alignment, the initial realignment was performed using a laser tracker (Leica AT-401 [12]). Figure 6 shows the displacement distributions of the accelerating structures in the horizontal direction before and after the initial realignment in the C5 straight section. A similar vertical displacement distribution was also obtained. The figure shows that the displacements of the

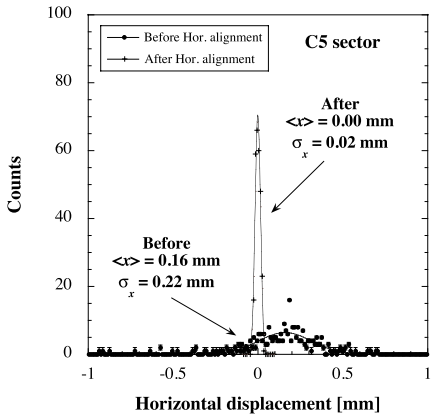

Figure 6: Horizontal displacement distributions of the accelerating structures before and after the initial realignment in the C5 straight section.

accelerating structures before the initial realignment have been more widely distributed in comparison with those after the realignment. The average displacements, $\langle x \rangle$ and $\langle y \rangle$, are 0.16 mm and -0.23 mm, respectively, and the distribution widths, σ_x and σ_y in one standard deviation, are 0.22 mm and 0.35 mm, respectively. The displacements have been successfully improved after the initial realignment, and the distribution widths, σ_x and σ_y, were improved to 0.02 mm and 0.07 mm, respectively. Currently, the initial realignment for most of the accelerating structures has been completed while that for quadruples is ongoing. The results of the initial realignment meets the alignment requirement for the injector linac.

Refinement in the alignment of the arc section

It is important to align magnets in the 180$^{\rm o}$ arc section with a high precision for preserving the emittacne of the electron beam. The alignment was improved by refining the connection condition of the arc to the two long straight sections. Here, the brief concept of the alignment procedure is described, and the technical description is given in detail elsewhere [13].

The arc comprises thirteen quadrupoles (seven quads inside the arc and six quads in the matching sections at both the ends of the arc), six sextupoles, and six bending magnets; the bending angle of the central magnets (2nd to 5th) is 30$^{\rm o}$ in the transverse plane, while it is 30$^{\rm o}$ + $\alpha/2$ for the outer magnets (1st and 6th). Because the two straight sections are not perfectly parallel but intersect at an angle of α, the outer bending magnets need to bend the beams by slightly larger angles. These magnets are arranged on a half circle with a diameter of 15 m, which should be smoothly connected to the two long straight sections in the transverse plane. The spatial arrangement of the arc section was redefined in both the rotational and vertical planes and the realignment was successfully performed after the redefinition by using the following alignment procedure.

In the vertical realignment procedure, vertical kinks of ∼0.05 mrad level at the inlet and outlet connections between the arc and two straight sections were successfully reduced, and the two straight sections were connected in alignment with the arc in the vertical direction. Here, the difference of ∼1 mm between the heights from the floor level of the inlet and outlet of the arc was corrected. In the transverse alignment procedure, the arc was rotated counterclockwise in the transverse plane by an angle of $\alpha/2 \sim$ 0.025 mrad, where the rotation center is set to the outlet point of the arc. As a result, the two straight sections were smoothly connected to the arc in each tangential direction at both the inlet and outlet connections. The alignment results of the bending magnets in the vertical direction and transverse plane are shown in fig. 7 and fig. 8, respectively. The first realignment for the arc section has been successfully completed. The displacements of all the magnets inside the arc were corrected in the vertical direction and transverse plane from 1.29 mm and 0.69 mm (rms), respectively, before the realignment to 0.57 mm and 0.07 mm (rms), respectively, after the realignment. The initial realignment of the arc section needs to be performed again because the results do not fully meet the alignment requirement.

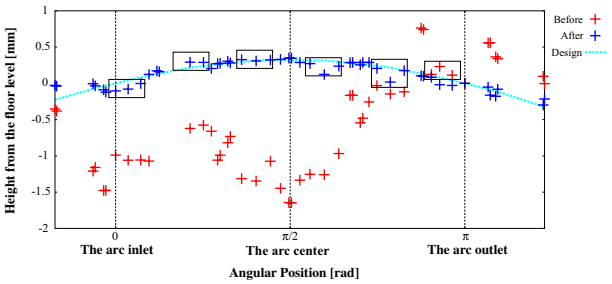

Figure 7: Variational plots of the alignment of the six bending magnets in the vertical direction. The red and blue crosses show data obtained before and after the alignment, respectively. The solid line (light blue) indicates the designed arrangement.

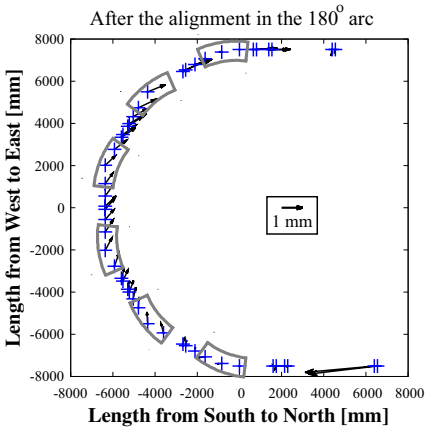

Figure 8: Variational plots (blue crosses) of the alignment of the six bending magnets in the transverse plane. The arrows indicate the residual displacements from the design.

Restoration of the accelerator girder unit

Because many girder units were heavily damaged because of the previous earthquake, their restoration with increased earthquake resistance is in progress. The girder units were initially designed in 1978 and fabricated in 1981–1982 at the injector linac. The fundamental design concept of the girder unit at that time had an earthquake-resistant structure to help mitigate stress concentration to the girder unit on the basis of its flexible structure. However, many girder units were still heavily damaged because the earthquake strength was far beyond our estimation.

Based on the spectral analyses for the previous earthquake, the frequency ranges are expected to spread over 2−12 Hz and 0.3−3 Hz for the response spectrum of acceleration and velocity of the ground surface, respectively. Strong resonances to the natural frequency of the earthquake can be avoided if the characteristic frequency of the girder unit is increased to more than 12 Hz. Thus, regarding the girder structure, we changed the initial design concept "flexible structure" to a new concept "rigid structure" to further increase the earthquake resistance. For this purpose, another support table was installed at the center of the girder unit to restrict the displacements in both the transverse and axial directions (see figs. 2 and 9).

Figure 9: New support table installed for restricting the displacements of the girder unit in both the transverse and axial directions.

To further increase the earthquake resistance, the thickness of the L-shaped plates of the girder unit was increased from 10 mm to 12 mm (see fig. 2). Based on the restoration, the characteristic frequencies were increased from 3 Hz to 13 Hz as shown in fig. 10 (a) and (b), respectively.

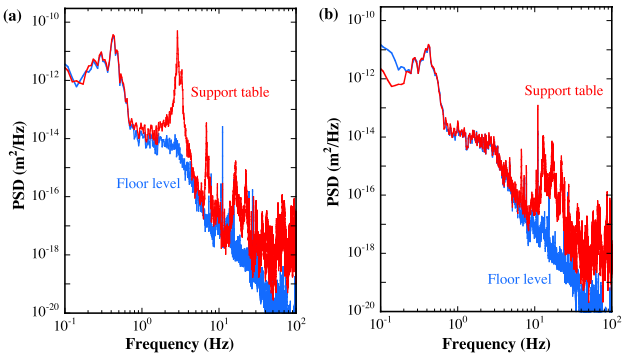

Figure 10: Variational plots of the power spectral density (PSD) of a girder unit as a function of vibration frequency (a) before and (b) after the restoration.

DYNAMICAL MOTION OF THE TUNNEL FLOOR AND FUTURE PROSPECTS

We observed the dynamical motion of the tunnel floor during the laser-based alignment measurements, although the present system is based only on static measurements. As a typical example, the variations in the vertical displacement of the girder units along the linac beam line are shown in fig. 11. The variational plots indicate the differential displacements obtained in the different dates. Similar variational plots were obtained for the horizontal direction. These differential displacements may be due to the dynamical motion of the floor level (or ground motion). The magnitude of the displacements is not negligible, and particularly, the displacements seem to be in certain systematic directions across expansion joints. Here, the expansion joints are buffer zones between adjacent building

blocks connected along the 500-m-long tunnel of the injector linac. The direct measurements of the dynamical motion of the building blocks are reported in detail elsewhere [13].

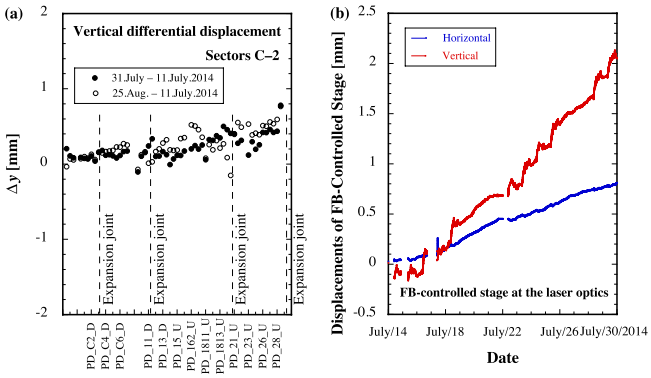

Figure 11: (a) Variational plots of the differential displacement of the girder units in the vertical direction along sectors C−2. The solid and open circles indicate the differential displacement obtained in the different dates, July 31 and August 25, respectively, with respect to the data recorded in July 11, 2014. (b) The horizontal (blue) and vertical (red) displacements of the feedback-controlled linear stages installed at the optical system as a function of date.

As another example, the dynamical displacements of the feedback-controlled linear stages in the transverse directions are shown in fig. 11. The laser fiducial is fixed at the center positions of the final QPD at the linac end during the laser-based alignment measurements under the feedback control; the injection angles of the laser fiducial can be automatically controlled at the optical system. The transverse displacements of the stages have been continuously recorded during the alignment measurements. The obtained data show the variations in the relative amount of the dynamical displacements of the stages in the transverse directions as a function of date. It is worth noting that the directions of the displacements seem to be constant during these dates. The behavior of the dynamical displacements are not simply sinusoidal; while they exhibit a slight daily variation due to tidal motion. The average rates of the variations are 0.05 and 0.13 mm/day in the horizontal and vertical directions, respectively, over 17 days.

The 500-m-long linac building comprises the tunnel floor (under the ground) and klystron gallery (on the ground), for which eight building blocks are connected in series with seven expansion joints. The expansion and contraction of each building block cannot be fully absorbed with these expansion joints, because of ground motion; thus, the residual non-absorptive deformation may cause certain amounts of deformation in the linac building, and this dynamical deformation may cause displacements of the floor level in the tunnel. If the dynamical deformation of each building block is independently caused, the fiducial points in the laser-based alignment system may be entirely missed, although the fiducial laser line is continuously fixed on the fiducial point at the linac end. Such phenomena may raise significant doubts regarding the reliability of the laser-based alignment technique. We are now preparing to investigate dynamical floor motion along the entire linac tunnel with computer-controlled movable QPDs.

SUMMARY

The initial realignment of the injector linac is successfully in progress towards the development of the SuperKEKB, for which the laser-based alignment system is now fully operational with a precision of less than 0.1 mm. The first realignment of the 180^{o} arc section was successfully completed. Many girder units were restored with improved earthquake resistance. The initial realignment of the accelerating structures on the girder units was nearly completed with a precision of 20 μm in one standard deviation and that of the quadrupole magnets is ongoing. We have started to fabricate remote-controlled QPDs because unexplainable dynamical motion of the tunnel floor was clearly observed during the alignment measurements.

ACKNOWLEDGMENT

The authors acknowledge K. Suzuki, N. Toyotomi, K. Kimura, Y. Mizukawa, T. Ichikawa, and S. Ushimoto of Mitsubishi Electric System & Service Co., Ltd. for their help with the measurements.

REFERENCES

[1] Y. Ohnishi, *et al.*, Prog. Theor. Exp. Phys. (2013) 03A011.

[2] T. Abe, *et al.*, Prog. Theor. Exp. Phys. (2013) 03A001.

[3] A. G. Akeroid, *et al.*, KEK Report 2009-12 (2010).

[4] M. Akemoto, *et al.*, Prog. Theor. Exp. Phys. (2013) 03A002.

[5] K. Furukawa, *et al.*, Proceedings of the 3rd International Particle Accelerator Conference (IPAC'13), Shanghai, China, 2013, pp. 1583–1585.

[6] T. Miura, *et al.*, Proceedings of the 4th International Particle Accelerator Conference (IPAC'14), Dresden, Germany, 2014, pp. 59–61.

[7] T. Natsui, *et al.*, Proceedings of the 3rd International Particle Accelerator Conference (IPAC'13), Shanghai, China, 2013, pp. 1117–1119; X. Zhou, *et al.*, *ibid.* pp. 2965–2967.

[8] T. Kamitani, *et al.*, Proceedings of the XXVIth International Linac Conference (LINAC'12), Tel-Aviv, Israel, 2012, pp. 177–179.

[9] N. Iida, *et al.*, Proceedings of the 2nd International Particle Accelerator Conference (IPAC'11), San Sebastian, Spain, 2011, pp. 2857–2861.

[10] T. Suwada, *et al.*, Rev. Sci. Instrum. 84, 093302 (2013).

[11] T. Suwada, *et al.*, Rev. Sci. Instrum. 81, 123301 (2010).

[12] http://http://www.leica-geosystems.com/en/index.htm.

[13] M. Tanaka, *et al.*, Proceedings of the 4th International Particle Accelerator Conference (IPAC'14), Dresden, Germany, 2014, pp. 1784–1786; *ibid.* pp. 1781–1783.